Modelling magnetised accretion discs

A. Brandenburg, C. Campbell

Department of Mathematics, University of Newcastle upon Tyne NE1 7RU, UK

Abstract Some recent results are reviewed that lead us now to believe that accretion discs are basically always magnetised. The main components are Balbus-Hawley and Parker instabilities on the one hand and a dynamo process on the other. A mechanical model for the Balbus-Hawley instability is presented and analysed quantitatively. Three-dimensional simulations are discussed, especially the resulting magnetic field structure. Possibilities of reproducing the field by an $\alpha\Omega$ dynamo are investigated, especially its symmetry with respect to the midplane.

1 Introduction

Until quite recently the origin of turbulence in accretion discs was considered to be rather obscure (see, for example, the excellent textbook by Frank et al 1992, Sect. 4.7). However, this seems to have changed considerably over the past few years. There is now strong numerical evidence that turbulence may be generated by the Balbus-Hawley instability (e.g. Hawley et al 1995, Matsumoto & Tajima 1995, Brandenburg et al 1995). Moreover, three-dimensional simulations show that even in the absence of an external magnetic field there will be self-excited turbulence, because the flow can regenerate the magnetic field by dynamo action (Brandenburg et al 1995, Hawley et al 1996, Stone et al 1996). We refer to this mechanism as dynamo-generated turbulence.

There remain several outstanding problems. Firstly, we need to gain a deeper understanding of how the dynamo process works. Is it some kind of an $\alpha\Omega$ dynamo, or is it something completely different? Secondly, what can we learn from local models of dynamo-generated turbulence if the real accretion disc is global? We begin by discussing briefly how keplerian shear flows become unstable in the presence of some coupling. We then consider the structure of large scale magnetic fields that might be generated in an accretion disc. Finally, we discuss the problem of global models of magnetised accretion discs.

2 A mechanical model of the instability

In order to understand the nature of the Balbus-Hawley (1991, 1992) instability it is useful to consider mechanical models displaying similar behaviour as a magnetised fluid in keplerian motion. An imposed uniform magnetic field, for example, holds the fluid particles in place like beads on an elastic string. In both cases there is a restoring force (with a given spring constant in the mechanical model, and the magnetic tension force in the hydrodynamical model). The

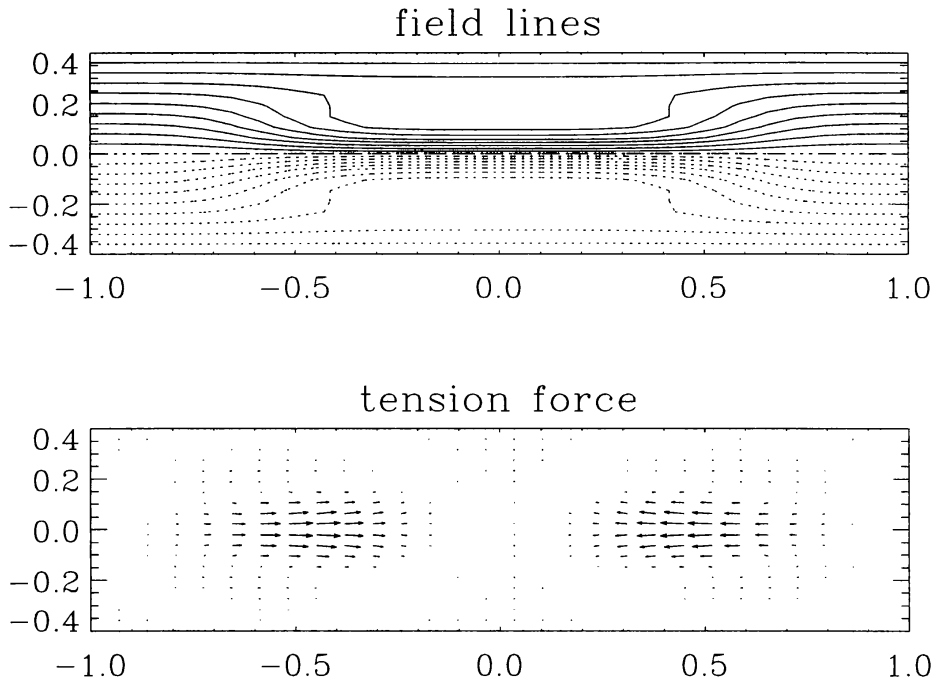

Fig. 1. Field lines representing a magnetic flux tube (upper panel). The Lorentz force $(\boldsymbol{\nabla}\times\boldsymbol{B})\times\boldsymbol{B}$ has no component in the direction of $\boldsymbol{B}$. However, the Lorentz force has two contributions, a magnetic pressure gradient, $-\frac{1}{2}\boldsymbol{\nabla}(\boldsymbol{B}^2)$, which is readily balanced by the gas pressure gradient, and the tension force, $(\boldsymbol{B}\cdot\boldsymbol{\nabla})\boldsymbol{B}$, which is plotted in the lower panel. The tension force tends to contract the tube. (In the thin flux tube approximation this contraction corresponds to a pressure gradient along the tube.)

analogy works also for nonuniform (turbulent) fields which typically consist of many flux tubes. Consider now a model with only two beads connected by a rubber band. This rubber band symbolises the restoring force experienced by a magnetic flux tube; see figure 1. The main difference is now that we can consider localized flux tubes and do not need to invoke a uniform large scale field. This seems more appropriate for characterizing turbulent magnetic fields as they seem to be present in the simulations. However, in this case the analogy is by no means exact, and yet it seems to capture some typical features of the dynamics of magnetic flux tubes.

Consider two particles in a keplerian orbit. The story is best conveyed with two space crafts orbiting round the earth and trying a rendezvous maneuver. *Larry November* from Sac Peak Observatory explained to us his memories of *Gemini 3 launched March 23, 1965 with Gus Grissom and John Young. The mission tried to dock with an Agena spacecraft launched separately and put into*

a similar orbit. The astronauts tried maneuvering by "eye" and were unable to close their gap with Agena because of the oddities of orbital dynamics. They found that they could not get closer by "speeding up". Increasing their orbital velocity only put them in a higher orbit which caused them to lag further beyond the Agena. The unsuccessful mission demonstrated that maneuvering spacecraft was unintuitive and could only be successful by use of computers. Subsequent missions used onboard computers to estimate crossing orbits given the relative locations of the spacecrafts. That software solution completely solved the difficultly and permitted entirely successful docking with the lunar excursion module with the mother Apollo craft used in all of the lunar landings. Of course software solutions could be accurate within millimeters and provide corrections that minimized expended fuel. It is surprising to hear that the astronauts really fell into this trap, but Larry also said *I do believe that after they realized the effect they did try breaking. Unfortunately, however, the effect is difficult to gauge and I do not think they were ever closer than about 100 m, and only managed to get hopelessly separated as they tried different things.* One should notice that the mission was allocated only 3 orbits, so this was probably not meant to be a particularly serious attempt!

Anyway, the main lesson is this: in order to go faster in a keplerian orbit one has to break, and vice versa. However, rubber bands behave more straightforwardly. They exert a restoring force when starting to pull. Therefore, objects in a keplerian orbit that are connected in some way always go unstable. In a sense this mechanism is reminiscent of *tidal disruption* of celestrial bodies passing nearby a black hole (see Novikov et al 1992). Here the restoring force is the self-gravity of the passing body. In fact, the criterion for disruption is similar to the stability criterion of Balbus-Hawley (see below).

In our simple model the positions of two coupled particles, $\boldsymbol{r}_1(t)$ and $\boldsymbol{r}_2(t)$, are governed by the equation

$$\ddot{\boldsymbol{r}}_i = -\frac{GM}{r^2}\hat{\boldsymbol{r}} - \boldsymbol{f}(\boldsymbol{r}_i - \boldsymbol{r}_j), \tag{1}$$

where G is the gravitational constant, M the mass of the central object, and $\boldsymbol{f}(\boldsymbol{x})$ is the restoring force in the direction $\hat{\boldsymbol{x}} = \boldsymbol{x}/|\boldsymbol{x}|$. The restoring force is assumed to be proportional to $|\boldsymbol{x}| - d_0$, where

$$d_0 = |\boldsymbol{r}_2(0) - \boldsymbol{r}_1(0)| \tag{2}$$

is the initial separation between the two particles. Thus, we put

$$\boldsymbol{f}(\boldsymbol{x}) = \begin{cases} K_0\hat{\boldsymbol{x}}(|\boldsymbol{x}| - d_0) & \text{when} \quad |\boldsymbol{x}| > d_0, \\ 0 & \text{otherwise.} \end{cases} \tag{3}$$

The cutoff for $|\boldsymbol{x}| < d_0$ was introduced to account for the fact that no force should be exerted when the rubber band is not tight, i.e. if the particles are too close together. The rubber band has a spring constant K_0 per unit mass, which is measured in units of $\Omega^2 = GM/r_0^3$, where Ω is the keplerian angular velocity at the initial radius r_0 of the particles.

In figure 2 we plot the positions of a pair of particles at different times for two different values of K_0. In the first case ($K_0 = \Omega^2$) the spring constant is weak enough so that the pair of particles becomes (tidally!) disrupted. However, in the second case ($K_0 = 10\Omega^2$) the coupling is strong enough so that the pair of particles always stays together. In addition to the counterclockwise orbital motion the two particles rotate about each other also in the counterclockwise direction.

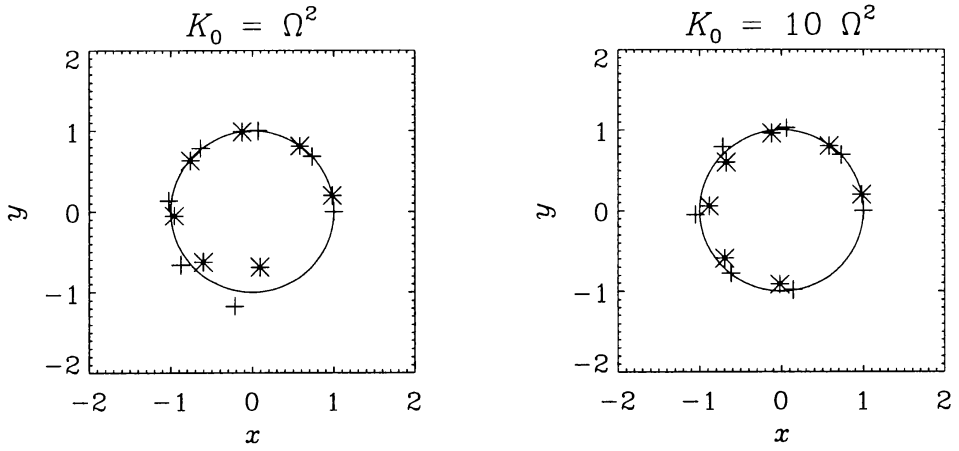

Fig. 2. The positions of a pair of particles at different times for two different values of K_0 (left panel: $K_0 = \Omega^2$, right panel $K_0 = 10\Omega^2$). Initially the leading particle (indicated by a star) moves inwards and the following particle (indicated by a plus) moves outwards.

This result can be understood by means of linear stability analysis. We assume $\boldsymbol{r}_i = \boldsymbol{r}_0 + \delta\boldsymbol{r}$, where $\boldsymbol{r}_0$ describes the motion of the center of mass with $\ddot{\boldsymbol{r}}_0 = -\Omega^2\delta\boldsymbol{r}_0$. Linearising the gravitational acceleration yields

$$\frac{GM}{r^2}\hat{\boldsymbol{r}} = \frac{GM}{(\boldsymbol{r}_0+\delta\boldsymbol{r})^3}(\boldsymbol{r}_0+\delta\boldsymbol{r}) = \Omega^2\boldsymbol{r}_0\left(1-3\frac{\delta\boldsymbol{r}\cdot\boldsymbol{r}_0}{r_0^2}\right)+\Omega^2\delta\boldsymbol{r}. \tag{4}$$

The linearised equation of motion is then

$$\delta\ddot{\boldsymbol{r}} = 3\Omega^2\frac{\delta\boldsymbol{r}\cdot\boldsymbol{r}_0}{r_0^2}-\Omega^2\delta\boldsymbol{r}+K\delta\boldsymbol{r}. \tag{5}$$

To get the dispersion relation we assume $\delta\boldsymbol{r}\propto e^{-i\omega t}$ and obtain after taking the inner product with $\boldsymbol{r}_0$

$$\omega^2 = -2\Omega^2+K. \tag{6}$$

The system is unstable when $\omega^2 < 0$, i.e.

$$K < 2\Omega^2 \quad \text{(instability)}. \tag{7}$$

We verified this also numerically. This dispersion relation is similar to the case of the Balbus-Hawley instability, where the criterion is:

$$\omega_A^2 < 2q\Omega^2 \quad \text{(instability)} \tag{8}$$

(Balbus & Hawley 1992), where $\omega_A = i\boldsymbol{k}\cdot\boldsymbol{B}/(4\pi\rho)^{1/2}$ is the Alfvén frequency for modes with wave vector $\boldsymbol{k}$ and $q \equiv -d\ln\Omega/d\ln r = 3/2$ for keplerian rotation. The criteria (7) and (8) are similar to the criterion of tidal disruption of celestrial bodies passing nearby a black hole

$$\omega_*^2 < \alpha^3\Omega^2 \quad \text{(instability)} \tag{9}$$

(Novikov et al 1992), where $\omega_* = GM_*/R_*^3$ is approximately the eigenfrequency of a star of mass M_* and radius R_* passing nearby the black hole. The coefficient α is of order unity. [Novikov et al (1992) quote the value 1.69 for an incompressible stellar model, see Kosovichev & Novikov (1991), but α is a little less for a polytropic stellar model, Luminet & Carter (1986)]. Common to all three cases is the fact that a harmonic oscillator with eigenfrequency ω can become overstable when placed in a keplerian orbit (or parabolic orbit in the case of tidal disruption) provided ω^2 is less than $\Omega^2 = GM/r_0^3$.

3 Dynamo generated turbulence

From the illustrative experiments above we have seen that both weak and strong coupling can lead to instability. A proper stability analysis of fluid in keplerian motion threaded by a magnetic field (of arbitrary orientation) confirm that there is indeed an instability (Balbus & Hawley 1991, 1992). The difference is that in the stability analysis there is a uniform imposed magnetic field, whereas the mechanical experiment presented here corresponds to an isolated magnetic flux tube connecting two points.

There are numerous subsequent investigations that extent the local analysis to global geometry (e.g. Curry et al 1994, Terquem & Papaloizou 1996, Ogilvie & Pringle 1996, Kitchatinov & Rüdiger 1997). We mentioned in the introduction that there are now also numerical simulations that show that the flow generated by the instability leads to turbulence, and that this turbulence in turn is capable of amplifying and sustaining the magnetic field by dynamo action. We briefly summarize here some of the basic results of such simulations.

The most significant result of such simulations is simply the fact that turbulence is self-sustained. An important quantitative outcome of the simulations concerns the strengths of the Maxwell and Reynolds stresses that would lead to mass accretion and angular momentum transport. Their magnitude is conveniently given in terms of the mean angular momentum gradient and a turbulent viscosity which, in turn, is specified in terms of natural units (sound speed c_s and disc scale height H) times a dimensionless factor, $\alpha_{\rm SS}$. Here the subscript SS

refers to Shakura & Sunyaev (1973), who introduced this concept in the context of accretion discs. Thus, the stress is expressed as

$$\langle m'_r u'_\phi - B'_r B'_\phi/4\pi \rangle = -\langle \rho \rangle \nu_t r \frac{\partial \Omega}{\partial r}, \quad \text{where} \quad \nu_t = \alpha_{\rm SS} c_s H. \tag{10}$$

where $m_r = \rho u_r$ is the mass flux in the radial direction and primes indicate fluctuations about the mean. The value of $\alpha_{\rm SS}$ fluctuates in time, because the system is turbulent and because the magnetic field varies strongly on long time scales. In figure 3 we show the evolution of the magnetic and kinetic contributions to $\alpha_{\rm SS}$. Comparison with the magnetic energy in the system shows that peaks in $\alpha_{\rm SS}$ coincide with peaks in the magnetic energy. On average the value of $\alpha_{\rm SS}$ is of the order of 0.01 (Brandenburg et al 1995, 1996a, Hawley et al 1996, Stone et al 1996). We should recall that some authors use a slightly different definition of $\alpha_{\rm SS}$, where $\alpha_{\rm SS}$ could be larger by a factor 3/2 times $\sqrt{2}$; (see the review by Brandenburg et al 1996b). Magnetohydrodynamic models of accretion discs (Campbell 1992, Campbell & Caunt 1996) show that such values of $\alpha_{\rm SS}$ are sufficient to lead to dynamically important large scale magnetic fields. The resulting $\langle B'_r B'_\phi \rangle$ stresses can play a major part in the radial advection of angular momentum necessary to drive the disc inflow. Note also that, although the field is oscillatory, $\langle B'_r B'_\phi \rangle$ is always negative.

The next important result of the simulations is that there could be long term variability of the dynamo activity, which is associated with a variable large scale field. In the cartesian models investigated by Brandenburg et al (1996a) the activity varies approximately cyclically with an average period of about 30 orbits. This varying large scale magnetic field, especially the toroidal component $\langle B_\phi \rangle$, strongly affects the value of $\alpha_{\rm SS}$ in a systematic manner which can be described by a parabolic fit of the form

$$\alpha_{\rm SS} \approx \alpha_{\rm SS}^{(0)} + \alpha_{\rm SS}^{(B)} \langle B_\phi \rangle^2 / B_{\rm eq}^2, \tag{11}$$

where $B_{\rm eq} = \langle 4\pi\rho c_s^2 \rangle^{1/2}$ is the equipartition value with respect to the *thermal* energy density, and $c_s = \Omega H/\sqrt{2}$ is the isothermal sound speed. (Both c_s and H depend on the disc temperature, which may change due to heating.) The most important contribution to (11) comes from the second term. In this second term the coefficient is $\alpha_{\rm SS}^{(B)} \approx 0.5$.

Another remarkable result concerns the dependence of the value of $\alpha_{\rm SS}$ on the rotation law. Abramowicz et al (1996) used the simulations for different values of $q \equiv -d\ln\Omega/d\ln r$. The value $q = 3/2$ is for keplerian rotation. Although the main parameter varied was q, Abramowicz et al expressed it in coordinate independent form using the magnitudes of the shear and vorticity tensors, σ and ω, respectively. They found that $\alpha_{\rm SS}$ varies approximately linearly with the ratio σ/ω. Abramowicz et al (1996) suggest that this result could be used in more general circumstances as well. This would be especially important if one were to produce a global accretion disc model. By this we mean a model, as opposed to a full three-dimensional turbulence simulation. The advantage of such a model

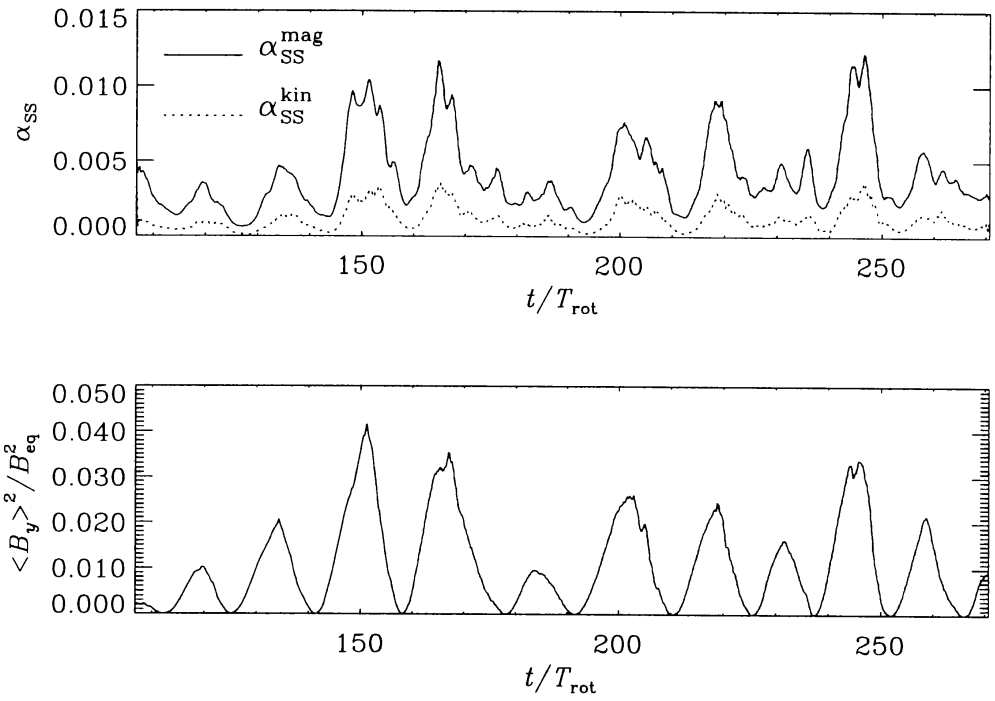

Fig. 3. Evolution of the magnetic and kinetic contributions to α_{SS}. Comparison with the magnetic energy of the mean field shows that peaks in α_{SS} coincide with peaks in the magnetic energy, which is plotted here in the form $\langle B_\phi \rangle^2 / B_{eq}^2$, where $B_{eq} = \langle 4\pi\rho c_s^2 \rangle^{1/2}$ is the equipartition value with respect to the *thermal* energy density, and $c_s = \Omega H/\sqrt{2}$ is the isothermal sound speed. The data are from Model O of the three-dimensional simulation of Brandenburg et al (1996a).

would be that it is easier to produce, and that it can be more easily applied to different circumstances. Before we consider this in more detail we need to discuss another complication that is related to the parameterization (10).

When we estimated the value of α_{SS} from eq. (10) we assumed that $\langle \rho \rangle$ was the *volume* averaged density. This seemed sensible, because the stresses do not strongly vary with height. However, it appears questionable whether a vertically averaged density would be a sensible description under more general circumstances, where the disc could be thick, for example. In that case it would seem natural to adopt an average that depends on height. However, this is not consistent with the numerical models, because then eq. (10) no longer represents a good description of the simulation's results, unless we relax the assumption that α_{SS} is independent of height.

We now allow α_{SS} to be height dependent. However, instead of assuming some unknown profile function we assume that this dependence is already captured by the dependence (11). Originally eq. (11) was obtained by considering

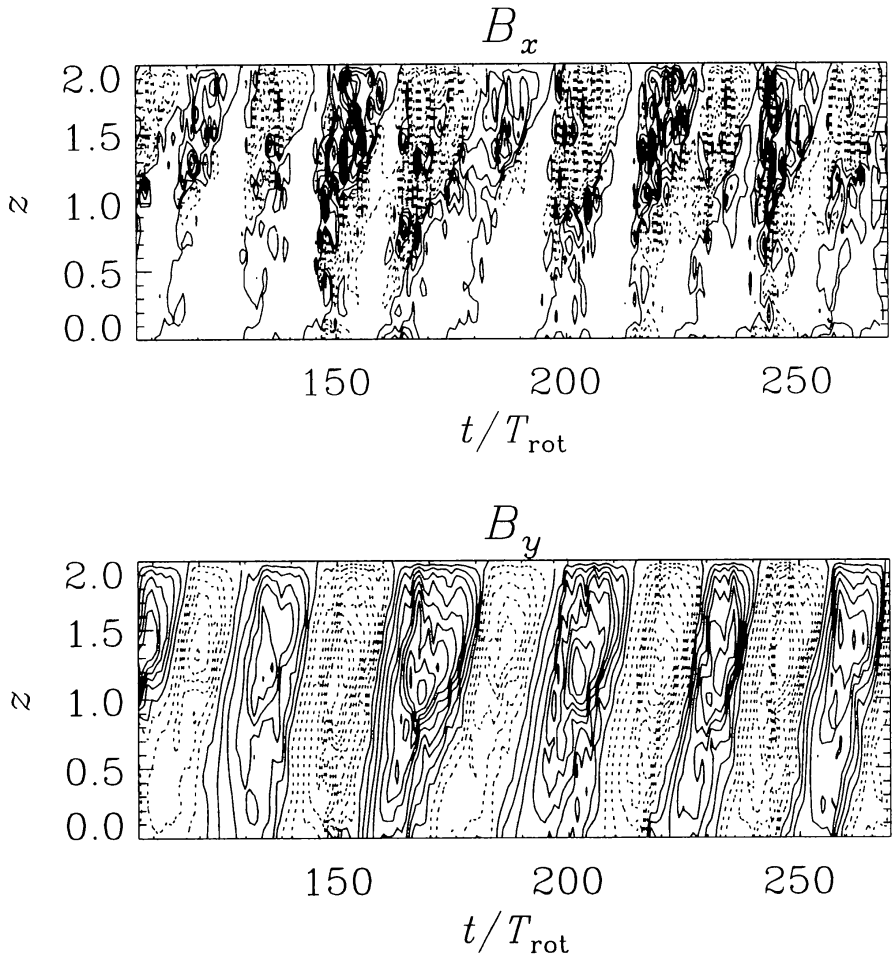

Fig. 4. Spatio-temporal pattern of the radial and toroidal components of the large scale field, $\langle B_x \rangle$ and $\langle B_y \rangle$, respectively, as a function of height and time. The data are from Model O of the three-dimensional simulation of Brandenburg et al (1996a).

volume averaged values of the stress and the density at different times during the magnetic cycle. We now assume that this relation is also valid at each height. Putting (11) into (10), and neglecting the $\alpha_{\rm SS}^{(0)}$ term, we find that the stress varies like

$$\text{stress} = -\frac{\alpha_{\rm SS}^{(B)} \langle B_\phi \rangle^2}{4\pi c_s^2} c_s H r \frac{\partial \Omega}{\partial r} = -\frac{\sqrt{2} q}{4\pi} \alpha_{\rm SS}^{(B)} \langle B_\phi \rangle^2, \tag{12}$$

which is now independent of $\langle \rho \rangle$. However, we have to know how $\langle B_\phi \rangle$ varies with height. So, if eq. (12) were to be used in an accretion disc model one would need a sensible prediction of the variation of the mean magnetic energy density with height. Unlike the local cartesian simulations, where the magnetic energy

density varied only little with height, in a truly global model the energy density ought to decrease as one goes sufficiently far away from the disc midplane. Thus, one is then seriously forced to consider accretion disc models that included the magnetic field evolution in a self-consistent manner. Let us now discuss how one can actually model the evolution of the mean magnetic field without invoking a full-blown numerical turbulence simulation. In order to appreciate the systematic behaviour of the large scale magnetic field we plot in figure 4 the spatio-temporal pattern of the radial and toroidal components of the large scale field, $\langle B_r \rangle$ and $\langle B_\phi \rangle$, respectively.

The large scale field, especially the toroidal magnetic field component, shows remarkable spatio-temporal coherence. The field varies not only cyclically, but it also migrates away from the midplane. The traditional approach to understand such organised behaviour is to adopt the mean-field approach, where the original induction equation is averaged and turbulent transport coefficients are introduced that describe the evolution of the nonlinear term, $\boldsymbol{\mathcal{E}} \equiv \langle \boldsymbol{u}' \times \boldsymbol{B}' \rangle$ in terms of the mean field itself. In principle such parameterizations can be fairly complicated, but more importantly, they are typically extremely uncertain. We may therefore use the simulations to estimate the "transport coefficients" assuming a relation $\boldsymbol{\mathcal{E}} = \boldsymbol{\mathcal{E}}(\langle \boldsymbol{B} \rangle)$. Such a relation should contain terms that are capable of yielding dynamo action. So, in its crudest approximation it should take the form

$$\langle \boldsymbol{u}' \times \boldsymbol{B}' \rangle = \alpha \langle \boldsymbol{B} \rangle - \eta_t \boldsymbol{\nabla} \times \langle \boldsymbol{B} \rangle, \tag{13}$$

where α is the traditional dynamo α-effect (not to be confused with $\alpha_{\rm SS}$) and η_t is a turbulent magnetic diffusivity. The simulations are consistent with the following estimates: $\alpha \approx -0.001 \Omega H$ and $\eta_t \approx 0.008 \Omega H^2$, where the sign of α is negative in the upper disc plane, but positive in the lower disc plane; see Brandenburg et al (1995), Brandenburg & Donner (1996). This is quite peculiar. The opposite result is expected from conventional mean-field theory, where the α-effect is related the helicity of the turbulence. Whilst the helicity of the turbulence in our simulations does have the expected sign, the simulations indicate that it has not much to do with α.

The sign of α can be explained as a direct consequence of the Balbus-Hawley instability. Figure 2 illustrates this. Initially this instability turns a toroidal magnetic flux tube in the counterclockwise direction. This is because the following particle accelerates, so it moves outwards, whilst the leading particle brakes and moves inwards, corresponding to counterclockwise rotation. This alone would not lead to an α-effect, or to a component of $\langle \boldsymbol{u}' \times \boldsymbol{B}' \rangle$ in the direction of $\langle \boldsymbol{B} \rangle$, because we also need a systematic orientation of the velocity. This bit is easy, however, because strong magnetic flux tubes are always susceptible to magnetic buoyancy, which will lift them vertically away from the midplane. So, motion in the direction of $\boldsymbol{z}$ together with a twist of the magnetic flux tube in the counterclockwise direction does lead to a systematic sign of the α-effect, and this sign is negative.

A negative α-effect has various implications. First of all, if the generated magnetic field is oscillatory, as in fact it is in the simulations, there will be a

magnetic field migration associated with its cyclic variation. This is indeed what is observed in the simulations. The direction of this field migration is indeed consistent with the implied negative sign of α. Furthermore, a negative α could affect parity selection of the magnetic field. While for positive α the preferred parity of the magnetic field is always even, this does not need to be the case when the sign of α is reversed. We address this in the following section.

To test the hypothesis that the magnetic field evolution seen in figure 4 can be explained by a mean-field dynamo we now solve the horizontally averaged induction equation using eq. (13),

$$\frac{\partial\langle B_x\rangle}{\partial t} = -\frac{\partial}{\partial z}\alpha\langle B_y\rangle + \eta_t\frac{\partial^2\langle B_x\rangle}{\partial z^2}, \tag{14}$$

$$\frac{\partial\langle B_y\rangle}{\partial t} = -q\Omega\langle B_x\rangle + \eta_t\frac{\partial^2\langle B_y\rangle}{\partial z^2}, \tag{15}$$

where $q = 3/2$. Here and below x corresponds to radius and y to longitude.) Since $\alpha \ll \Omega H$ we have neglected the α-effect in the second equation (15). On the boundaries we assume

$$\frac{\partial\langle B_x\rangle}{\partial z} = \frac{\partial\langle B_y\rangle}{\partial z} = 0 \quad \text{on} \quad z = 0; \quad \langle B_x\rangle = \langle B_y\rangle = 0 \quad \text{on} \quad z = L_z. \tag{16}$$

This boundary condition was also used in the three-dimensional simulations (except in those cases where no symmetry was prescribed; see figure 6). The calculations of Brandenburg et al (1995) confirmed that α changes sign about the equator. The simplest functional form for α is therefore $\alpha = \alpha_0(z/H)$. For $\alpha_0 = -0.001\Omega H$ we reproduce the right cycle frequency, $\Omega_{\rm cyc}/\Omega = 0.03$. In fact, one can show that $\Omega_{\rm cyc}/\Omega = \mathcal{O}(|\alpha/\Omega H|^{1/2})$. In figure 5 we plot the resulting spatio-temporal pattern of $\langle B_x\rangle$ and $\langle B_y\rangle$. The qualitative agreement with figure 4 is quite striking.

4 The parity of large scale magnetic fields

A large number of different dynamo models has been studied over the years. However, the case of a negative α-effect has not received much attention, because it was thought to be unphysical. In the case of galactic dynamos the result is typically that for $\alpha_0 < 0$ oscillatory modes of dipole-type parity are most easily excited (Parker 1971, Stix 1975, see also Brandenburg et al 1990). This result is interesting in various respects. Firstly, a dipole-like magnetic field seems to be more favourable when modelling magnetically driven jets from accretion discs (eg Yoshizawa & Yokoi 1993 and references therein). However, if a dipole-like magnetic field is indeed easier to excite than a quadrupole-like magnetic field the question arises why the field found in the local simulations was actually still quadrupole-like. Also, although galactic dynamos are similar in geometry to accretion disc dynamos, there are marked differences concerning especially the form of the rotation curve. So we are encouraged to look now more systematically at the different field parities under those different conditions.

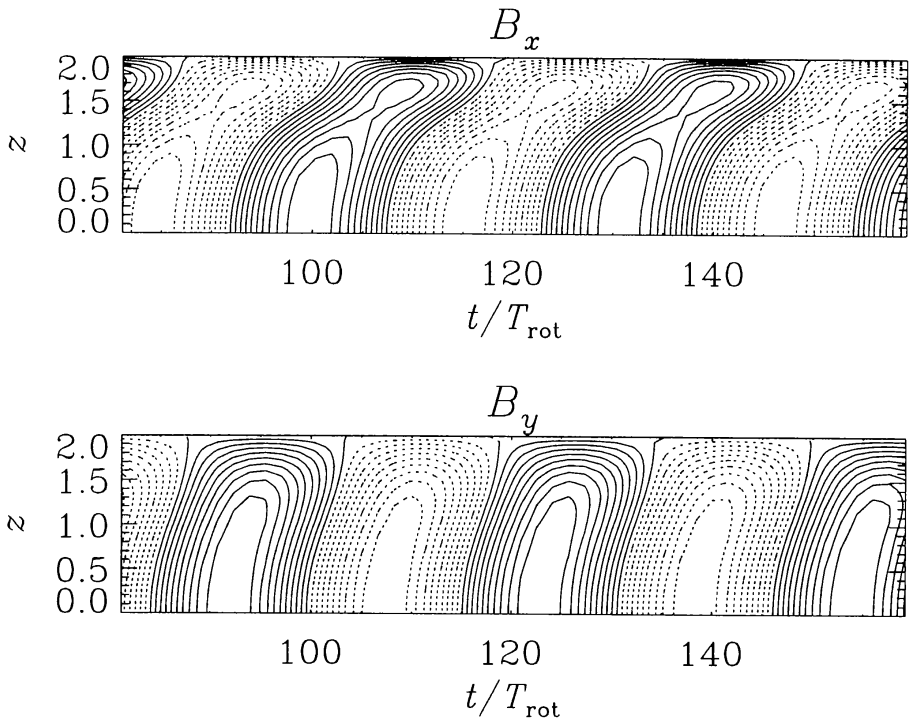

Fig. 5. Spatio-temporal pattern of $\langle B_x \rangle$ and $\langle B_y \rangle$ as a function of height and time, obtained by solving (14)-(16).

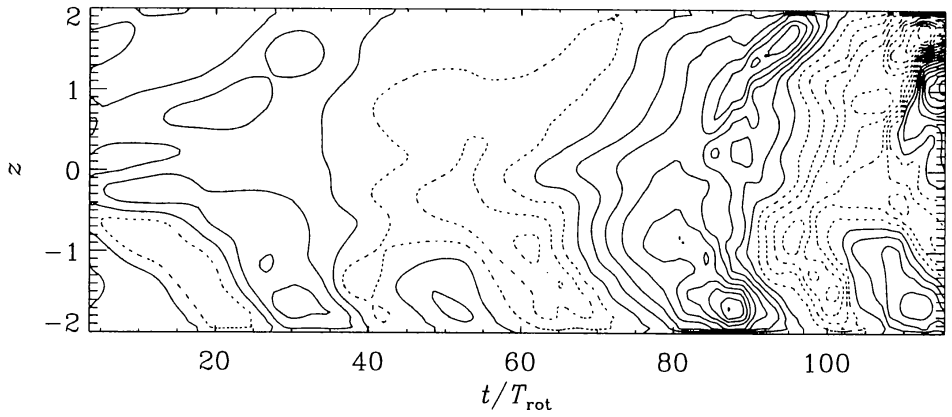

Fig. 6. Spatio-temporal pattern of $\langle B_y \rangle$ as a function of height and time for the three-dimensional simulation of Brandenburg et al (1995). No restriction to the parity is made. Note that the field is mostly symmetric about the midplane.

First we consider the magnetic field generated by a mean-field dynamo in a local box with the same boundary conditions as those used in the numerical simulations. The field structure of $\langle B_x \rangle$ and $\langle B_y \rangle$ is given in figure 7. The critical values of the dynamo number

$$D = q\frac{\alpha_0 \Omega_0 H^3}{\eta_t^2} = q\left(\frac{\alpha_0}{\Omega_0 H}\right)\left(\frac{\eta_t}{\Omega_0 H^2}\right)^{-2}, \tag{17}$$

where the dynamo is just marginally supercritically, are given in table 4. Here, $q = 3/2$ for keplerian rotation. Note that even for negative α the quadrupole-type geometry (even parity) is the most preferred one. This is a bit surprising, but it is at least not in conflict with the results of the three-dimensional simulations, which also give quadrupole-type symmetry when no symmetry restriction is imposed; see figure 6. Continuous inflow through the disc requires a quadrupole-type field structure. Unless the surroundings are very highly conducting, a dipole-type field does not lead to a magnetic torque on rings of disc material and hence cannot contribute to the radial advection of angular momentum (Campbell 1997).

However, we now need to check whether the occurrence of a quadrupole mode for negative values of α could be an artefact of the local geometry used in our model. Therefore we now consider briefly a global $\alpha\Omega$ dynamo model with a disc-like distribution of α and η_t. In this model we used the following profiles for α and Ω

$$\alpha = \alpha_0 \frac{z}{H} \exp\left\{\frac{1}{2}\left[1 - \left(\frac{z}{H}\right)^2\right]\right\}, \tag{18}$$

$$\Omega = \Omega_0 \left[1 + \left(\frac{r}{r_0}\right)^{\frac{3}{2}n}\right]^{\frac{1}{n}}, \tag{19}$$

with $n = 10$. Again, the result is surprising. The critical solutions are plotted in figure 7 and the critical values of the dynamo number D are given in table 4, where we also compare with results obtained by other authors.

The table shows that there is not a unique result regarding the parity of the easiest excited mode for negative values of α. The disks of Stepinski & Levy (1988, SL88) are relatively thick and represent only this innermost parts of the disc. The general behaviour of those models is similar to dynamos in spherical geometry. The models of Stepinski & Levy (1990, SL90) are thinner, and here the parity depends on whether the fields are confined to the disc (SL90-1) or whether the disc is surrounded by a vacuum (SL90-2), permitting the field to extend into the corona. In Torkelsson & Brandenburg (1994a, TB94) the parity depends on whether or not there is a cavity in the middle of the disc. In those models a cavity was introduced to model an inner boundary of the disc at the innermost stable orbit around black holes. If such a cavity is present (TB94-4c, ie Model c in their Table 4), then A0 parity is more preferred.

To shed some light on the occurrence of the different modes we now compute the full spectrum of growth rates shown as a function of dynamo number $D =$

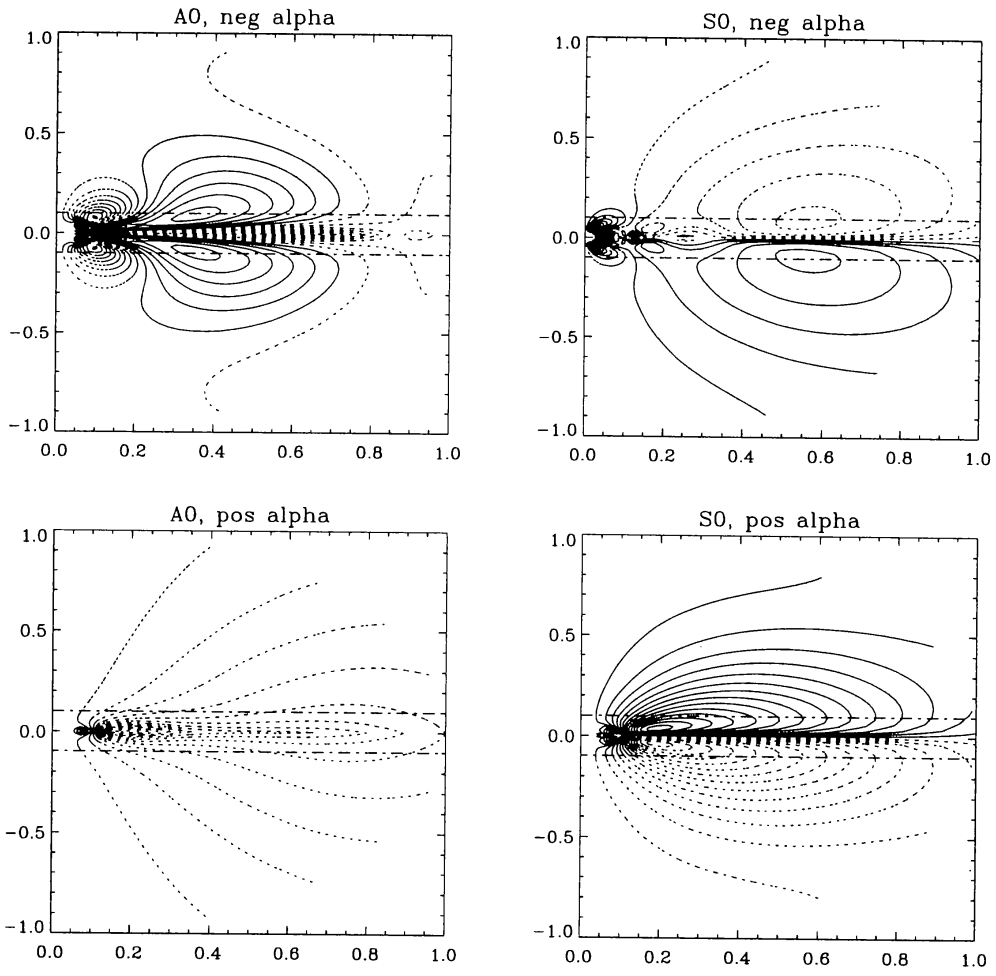

Fig. 7. Poloidal magnetic field (dotted lines indicate opposite field orientation) for an $\alpha\Omega$ dynamo in disc-like geometry using the profiles given by (18) and (19).

$q\alpha_0\Omega_0 H^3/\eta_t^2$ by solving an eigenvalue problem; see figure 8. Again we use $\alpha = \alpha_0(z/H)$. Note that for either sign of D the growth rates of quadrupole-like (symmetric or S0) solutions are largest. Those modes are oscillatory, except for a certain interval $0 < D \lesssim 400$ (positive alpha, but negative shear), where this branch splits into two non-oscillatory branches. Similar behavior is seen for the next easily excited mode of A0 type (antisymmetric), but here the two non-oscillatory solutions have merged into a single oscillatory one before its growth rate becomes positive. This illustrates where the sensitivity of either oscillatory or non-oscillatory behaviour comes from.

In conclusion, we must regard the parity of the dynamo as uncertain: it depends on geometrical aspects which could decide upon whether or not two non-

Table 1. Critical values of the dynamo number for different models (see text for explanations). Numbers in bold face indicate the most easily excited mode. A0 and S0 refer to antisymmetric (dipole-type) and symmetric (quadrupole-type) modes.

	neg alpha		pos alpha	
	A0	S0	A0	S0
cartesian	−1130 osc	**−400** osc	+630 osc	**+13** st
Figure 7	−130 osc	**−80** osc	+160 osc	**+35** osc
TB94-4O	−576 osc	**−512** osc	+352 osc	**+40** st
TB94-4c	**−1080** osc	−1120 osc	+792 osc	**+77** st
SL88-3	**−138** osc	−169 osc	+201 osc	**+187** osc
SL90-1	**−9** st	−45 osc	**+40** osc	+60 st
SL90-2	−68 osc	**−45** st	+48 osc	**+9** st

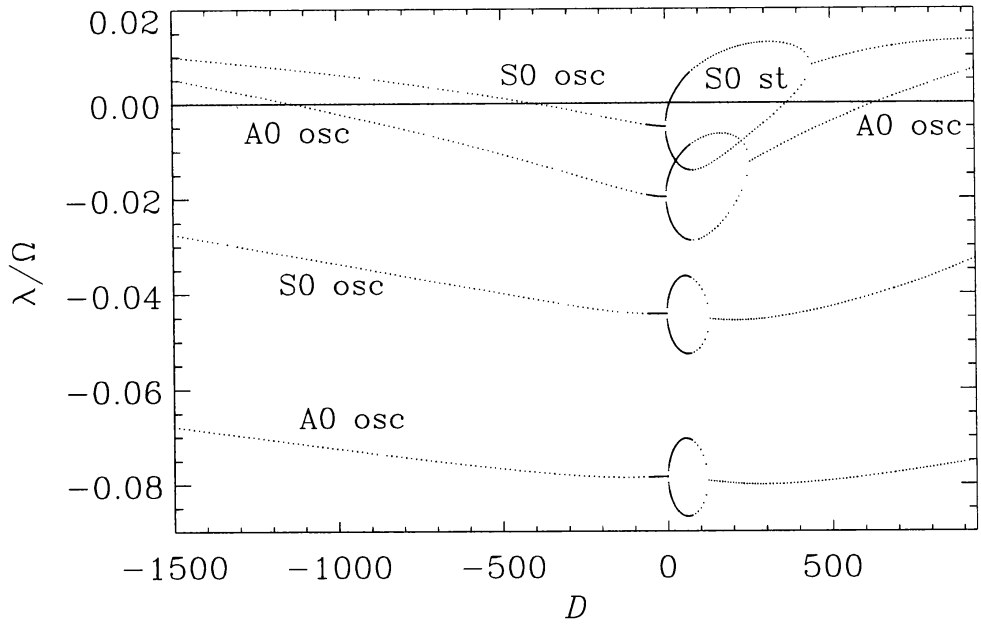

Fig. 8. Growth rates λ (in units of Ω) as a function of the dynamo number D for a dynamo in cartesian geometry using equations (14) and (15) and $\alpha = \alpha_0 z/H$ in $0 < z < H$.

oscillatory branches have merged into a single oscillatory one. Also, in the highly nonlinear regime things can change again, as was demonstrated by Torkelsson & Brandenburg (1994b), who presented a survey of models for both signs of α, different nonlinearities (buoyancy and α-quenching), and a large range of different dynamo numbers.

5 Towards a magnetised standard disc model

In the forthcoming years it will be important to design a new standard accretion disc model that includes those new effects turbulence simulations have revealed recently. Ideally, one would like to have a magnetic version of the famous Shakura-Sunyaev solution. The model by Campbell (1992) is such an example. In this section we briefly address a few issues where some adjustments to this theory could be made and where conceptual differences should need some further clarification.

An important property of the dynamo is the value of the magnetic field at which the dynamo saturates. This value is determined by the dominant feedback magnetism. In the model of Campbell (1992) it was assumed that magnetic buoyancy limits the magnetic field strength. Another possibility is α-quenching, which seems to be important in the three-dimensional simulations (Brandenburg & Donner 1996). A more urgent concern is related to the sign of the dynamo α. The simulations suggest that α is negative. This is rather surprising and could not have been predicted. This appears to be directly related to the dynamics of the Balbus-Hawley instability. So we do have some understanding of this surprising result and are tempted to include it into actual models of magnetised accretion discs. One immediate consequence would be that the magnetic field can no longer assumed to be steady. A variable level of the magnetic field could lead to variability of the temperature in the disc, which could be of interest in connection with the outbursts of cataclysmic variables (CVs). Current models describing outbursts of CVs invoke a dependence of $\alpha_{\rm SS}$ on H/R (e.g. Cannizzo et al 1988), which does not seem to be supported by the simulations (Vishniac & Brandenburg 1997). Furthermore, standard outburst models require $\alpha_{\rm SS}$ to be around 0.1 during outbursts. Such a large value could only be achieved in the presence of a sufficiently strong magnetic field. This seems unsatisfactory, because the origin of such a field needs to be explained. More importantly, it would then be difficult to explain the absence of strong fields during quiescent phases. Therefore a self-consistent model for CV outbursts seems to be highly desirable.

6 Conclusions

Significant progress has been made in understanding the origin of viscosity and the nature of turbulence in accretion discs. Three-dimensional simulations in local geometry can be used to address those questions. Nevertheless, it is important to consider those simulations as preliminary. Global simulations using more realistic, open, boundary conditions and including the effects of curvature are necessary. Finally, proper account of radiative transfer should be made before we can begin to address questions of observational significance, such as the CV outbursts.

References

Abramowicz, M. A., Brandenburg, A., & Lasota, J.-P. 1996 *Monthly Notices Roy. Astron. Soc.* **281**, L21-L24.

Balbus, S. A. & Hawley, J. F. 1991 *Astrophys. J.* **376**, 214-222.

Balbus, S. A. & Hawley, J. F. 1992 *Astrophys. J.* **400**, 610-621.

Brandenburg, A. & Donner, K. J. 1996 *Monthly Notices Roy. Astron. Soc.* (submitted).

Brandenburg, A., Tuominen, I., Krause, F. 1990 *Geophys. Astrophys. Fluid Dyn.* **50**, 95-112.

Brandenburg, A., Nordlund, Å., Stein, R. F., Torkelsson, U. 1995 *Astrophys. J.* **446**, 741-754.

Brandenburg, A., Nordlund, Å., Stein, R. F., Torkelsson, U. 1996a *Astrophys. J. Letters* **458**, L45-L48.

Brandenburg, A., Nordlund, Å., Stein, R. F., Torkelsson, U. 1996b Dynamo generated turbulence in disks: value and variability of alpha. In *Physics of Accretion Disks* (ed. S. Kato et al) pp.285–290. Gordon and Breach Science Publishers.

Campbell, C. G. 1992 *Geophys. Astrophys. Fluid Dyn.* **63**, 197-213.

Campbell, C. G. 1997 *Magnetohydrodynamics in Binary Stars.* Kluwer Academic Publishers, Dordrecht.

Campbell, C. G. & Caunt, S. E. 1996 *Mon. Not. R. Astr. Soc.*, submitted.

Cannizzo, J. K., Shafter, A. W., Wheeler, J. C. 1988 *Astrophys. J.* **333**, 227-235.

Curry, C., Pudritz, R. E., & Sutherland, P. 1994 *Astrophys. J.* **434**, 206-220.

Frank, J., King, A. R., & Raine, D. J. 1992 *Accretion power in astrophysics.* Cambridge: Cambridge Univ. Press.

Hawley, J. F., Gammie, C. F., & Balbus, S. A. 1995 *Astrophys. J.* **440**, 742-763.

Hawley, J. F., Gammie, C. F., & Balbus, S. A. 1996 *Astrophys. J.* **464**, 690-703.

Kitchatinov, L. L. & Rüdiger, G. 1997 *Monthly Notices Roy. Astron. Soc.* (in press).

Kosovichev, A. G. & Novikov, I. D. 1991 Preprint IOA, Cambridge.

Luminet, J.-P. & Carter, B. 1986 *Astrophys. J. Suppl.* **61**, 219-248.

Matsumoto, R. & Tajima, T. 1995 *Astrophys. J.* **445**, 767-779.

Novikov, I. D., Pethick, C. J. & Polnarev, A. G. 1992 *Monthly Notices Roy. Astron. Soc.* **255**, 276-284.

Ogilvie, G. I. & Pringle, J. E. 1996 *Monthly Notices Roy. Astron. Soc.* **279**, 152-164.

Parker, E. N. 1971 *Astrophys. J.* **163**, 255-278.

Shakura, N. I., & Sunyaev, R. A. 1973 *Astron. Astrophys.* **24**, 337-355.

Stepinski, T. F., Levy, E. H. 1988 *Astrophys. J.* **331**, 416-434.

Stepinski, T. F., Levy, E. H. 1990 *Astrophys. J.* **362**, 318-332.

Stix, M. 1975 *Astron. Astrophys.* **42**, 85-89.The galactic dynamo Erratum: A&A 68,459

Stone, J. M., Hawley, J. F., Gammie, C. F., & Balbus, S. A. 1996 *Astrophys. J.* **463**, 656-671.

Terquem, C. & Papaloizou, J. C. B. 1996 *Monthly Notices Roy. Astron. Soc.* **279**, 767-784.

Torkelsson, U. & Brandenburg, A. 1994a *Astron. Astrophys.* **283**, 677-691.

Torkelsson, U. & Brandenburg, A. 1994b *Astron. Astrophys.* **292**, 341-349.

Vishniac, E. T. & Brandenburg, A. 1997 *Astrophys. J.* **475**, -.

Yoshizawa, A., Yokoi, N. 1993 *Astrophys. J.* **407**, 540-548.